

# Effects of Transient Receptor Potential-Like Current on the Firing Pattern of Action Potentials in the Hodgkin-Huxley Neuron during Exposure to Sinusoidal External Voltage

Bing-Shuo Chen<sup>1, 2, 3</sup>, Yi-Ching Lo<sup>4</sup>, Yen-Chin Liu<sup>5</sup>, and Sheng-Nan Wu<sup>2, 6</sup>

<sup>1</sup>Department of Anesthesiology, Buddhist Dalin Tzu Chi General Hospital, Chiayi

<sup>2</sup>School of Medicine, Tzu Chi University, Hualien

<sup>3</sup>Institute of Basic Medical Sciences, National Cheng Kung University Medical College, Tainan

<sup>4</sup>Department of Pharmacology, Kaohsiung Medical University, Kaohsiung

<sup>5</sup>Department of Anesthesiology, National Cheng Kung University Medical College, Tainan  
and

<sup>6</sup>Department of Physiology, National Cheng Kung University Medical College, Tainan  
Taiwan, Republic of China

## Abstract

Transient receptor potential vanilloid-1 (TRPV1) channels play a role in several inflammatory and nociceptive processes. Previous work showed that magnetic electrical field-induced antinociceptive action is mediated by activation of capsaicin-sensitive sensory afferents. In this study, a modified Hodgkin-Huxley model, in which TRP-like current ( $I_{TRP}$ ) was incorporated, was implemented to predict the firing behavior of action potentials (APs), as the model neuron was exposed to sinusoidal changes in externally-applied voltage. When model neuron is exposed to low-frequency sinusoidal voltage, increased maximal conductance of  $I_{TRP}$  can enhance repetitive bursts of APs accompanied by a shortening of inter-spike interval (ISI) in AP firing. The change in ISIs with number of interval is periodic with the phase-locking. In addition, increased maximal conductance of  $I_{TRP}$  can abolish chaotic pattern of AP firing in model neuron during exposure to high-frequency voltage. The ISI pattern is converted from irregular to constant, as maximal conductance of  $I_{TRP}$  is increased under such high-frequency voltage. Our simulation results suggest that modulation of TRP-like channels functionally expressed in small-diameter peripheral sensory neurons should be an important mechanism through which it can contribute to the firing pattern of APs.

**Key Words:** Hodgkin-Huxley model, transient receptor potential (TRP), action potential, computer simulations

## Introduction

Ion channels can be thought to have gates that regulate the permeability of the pore to ions. These gates can be controlled by membrane potential, producing voltage-gated channels, by chemical ligands, producing ligand-gated channels, or by a combination of factors. Voltage- or ligand-gated ion channels and

the currents that flow through them are able to underlie much of the electrical behavior of cells (7).

Capsaicin-sensitive, transient receptor potential vanilloid-1 (TRPV1) receptor-expressing sensory nerves are recognized to play an important role in several inflammatory and nociceptive processes via the release of pro-inflammatory/pro-nociceptive sensory neuropeptides such as substance P and calcitonin

gene-related peptide into the innervated area (1, 2, 5, 11, 20). The TRPV1 receptor is a non-selective cation channel, which is activated by exogenous vanilloid compounds (*e.g.*, capsaicin or resiniferatoxin), as well as noxious heat and several endogenous chemical stimuli, such as protons, bradykinin, and leukotrienes produced in the inflamed tissues (5, 10, 20). A recent study showed experimental evidence for the involvement of capsaicin-sensitive sensory nerves in the optimized static magnetic field-induced anti-nociceptive action (14). However, the precise mechanism through which the activation of TRPV1 receptor is responsible for such anti-nociceptive action remains largely unknown.

Over the past decade, a role for transient receptor potential (TRP)-like channels in temperature sensation has emerged (11). TRPV1, a subset of TRP-like channels, is a nonselective ligand-gated cation channel that may be activated by a variety of exogenous and endogenous stimuli, including heat greater than 43°C, low pH, anadamide, and capsaicin. TRPV1 can act physiologically as a transducer of noxious heat, as well as a detector of capsaicin, acid, and arachidonic acid metabolites (5, 11). TRPV1 receptors are involved in the transmission and modulation of pain, as well as the integration of diverse painful stimuli. Through binding to these receptors, capsaicin can selectively activate A $\delta$  and C fibers, which transmit nociceptive information to the spinal cord. The importance of TRPV1 channels in peripheral sensitization was demonstrated in vanilloid receptor-1-null mice (1, 5).

Effect of temperature change on electrical behavior in modeled skin neuron has been recently simulated (12). Electrical stimulation with different frequencies was also experimentally reported to induce neuropeptide release (6). However, whether the activity of TRP-like channels contributes to electrical firing thus far has not been explored. Therefore, in this study, we used a simulation approach to the evaluation of the role of TRP-like current in generation of neuronal firing in a model neuron exposed to sinusoidal voltage with varying frequency. The firing of action potentials (APs) was modeled using the Hodgkin-Huxley (HH) formalism of squid axon excitability not only for convenience but because this conductance-based model of neural systems has been well established and tested at our laboratory (8, 16, 17, 19).

## Materials and Methods

To simulate firing of capsaicin-sensitive sensory neuron in this study, a Hodgkin-Huxley (HH) type model (8, 17, 19) was mathematically constructed. In addition, TRP-like current is included, given that this current is functionally expressed in sensory neuron

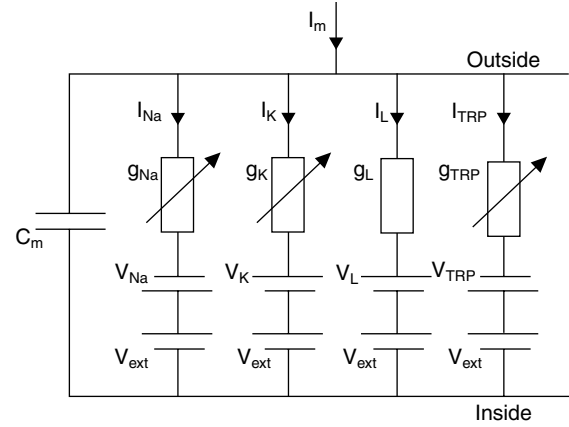


Fig. 1. Circuit model corresponding to a modified HH model exposed to external electrical field ( $V_{ext}$ ). Notably, a TRP-like current is also included.

(2, 5, 10, 20). Because these types of channels identified thus far are nonselective cation ion channels (5, 10), their reversal potential was assumed to be nearly zero. The circuit model used in this study is illustrated in Fig. 1. Ion currents were modeled according to the HH kinetic scheme:

$$C_m \frac{dV}{dt} = -[\bar{g}_{Na} m^3 h (V + V_{ext} - V_{Na}) + \bar{g}_K n^4 (V + V_{ext} - V_K) + g_L (V + V_{ext} - V_L) + \bar{g}_{trp} (V + V_{ext} - V_{trp})] + I_{app},$$

$$\frac{dm}{dt} = \alpha_m(V)(1 - m) - \beta_m(V)m,$$

$$\frac{dh}{dt} = \alpha_h(V)(1 - h) - \beta_h(V)h,$$

$$\frac{dn}{dt} = \alpha_n(V)(1 - n) - \beta_n(V)n,$$

where  $V$  is the membrane potential,  $C_m$  the membrane capacitance and  $t$  the time (msec).  $\bar{g}_{Na}$ ,  $\bar{g}_K$ , and  $\bar{g}_{TRP}$  represent the maximal conductance of inward  $Na^+$  current ( $I_{Na}$ ), outward  $K^+$  current ( $I_K$ ), and TRP-like current ( $I_{TRP}$ ), respectively, and  $g_L$  leak current conductance.  $I_{app}$  is the externally-applied current injected into the cell and  $V_{ext}$  sinusoidal voltage with varying frequencies. The dimensionless gating variables are denoted by  $m$ ,  $h$ , and  $n$  respectively. Gating variable dynamics are modeled as the solution of the first-order ordinary differential equation.  $Na^+$  current conductance is modeled using  $m^3 h$  formalism, whereas  $K^+$  current conductance using  $n^4$  formalism (8, 16, 19).  $\alpha_y(V)$  and  $\beta_y(V)$  ( $y = m, h, n$ ) represent nonlinear function of  $V$ .

The rate constants used in the simulation were, for  $I_{Na}$ :

**Table 1. Default parameter values used for the modified HH model used in this study**

Symbol	Description	Value
$C_m$	Membrane capacitance	1 $\mu\text{F}$
$\bar{g}_{Na}$	Maximal $\text{Na}^+$ current conductance	120 $\text{mS}/\text{cm}^2$
$\bar{g}_K$	$\text{K}^+$ current conductance	30 $\text{mS}/\text{cm}^2$
$g_L$	Leak current conductance	0.3 $\text{mS}/\text{cm}^2$
$\bar{g}_{TRP}$	TRP-like current conductance*	0.03 $\text{mS}/\text{cm}^2$
$V_{Na}$	$\text{Na}^+$ reversal potential	50 mV
$V_K$	$\text{K}^+$ reversal potential	-80 mV
$V_L$	Reversal potential for leak current	-49 mV
$V_{TRP}$	Reversal potential for TRP-like current	0 mV

\*TRP: transient receptor potential

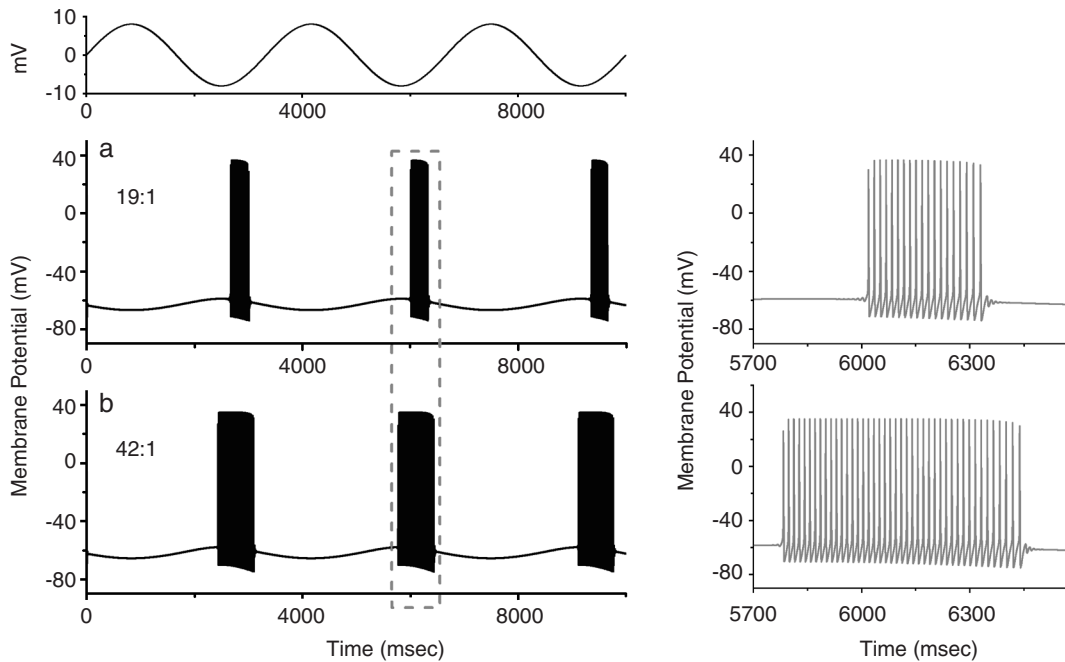


Fig. 2. Simulation used to study effect of  $I_{TRP}$  on the firing of APs in modified HH model. The amplitude and frequency of external voltage were set to be 8 mV and 0.3 Hz, respectively. In (a) and (b), the maximal conductance of  $I_{TRP}$  (i.e.,  $\bar{g}_{TRP}$ ) is 0.03 and 0.06  $\text{mS}/\text{cm}^2$ , respectively. The uppermost part denotes sinusoidal voltage with a frequency of 0.3 Hz applied to the model. For the sake of clarity, the inset shown in the rightmost side indicates expanded time scale of potential traces (dashed box). Notably, entrainment pattern of 19:1 and 42:1 is shown in (a) and (b), respectively. There are 19 and 42 APs generated for one cycle stimulation in (a) and (b), respectively.

$$\alpha_m = 0.1(V + 40)/\{1 - \exp[-0.1(V + 40)]\},$$

$$\beta_n = 0.125\exp[-0.0125(V + 65)],$$

$$\beta_m = 4\exp[-0.055(V + 65)],$$

and for  $I_{TRP}$ :

$$\alpha_h = 0.07\exp[-0.05(V + 65)],$$

$$I_{trp} = \bar{g}_{TRP}(V + V_{ext} - V_{TRP}).$$

$$\beta_h = 1/\{1 + \exp[-0.1(V + 55)]\},$$

for  $I_K$ :

$$\alpha_n = 0.01(V + 55)/\{1 - \exp[-0.1(V + 55)]\},$$

$V_{ext}$  was generated using the equation:  $V_{ext} = V_A \sin(2\pi \times f \times t)$ , where  $V_A$  and  $f$  are amplitude and frequency of sinusoidal external voltage, respectively. Simulations presented here were performed using Euler algorithm as implemented in Microsoft Excel

(3, 19) or in the program XPP with the aid of the X-Win32 version of XPPAUT on a Hewlett Packard Workstation (HP xw9300; Palo Alto, CA) or on a LINUX workstation (4, 16, 18). XPPAUT is a tool for solving differential equations, difference equations, delay equations, functional equations, boundary value problems, and stochastic equations. The program code can bring together a number of useful algorithms and be portable. The information for XPP software is readily available at <http://www.math.pitt.edu/~bard/XPP/XPP.html>. The conductance values and reversal potentials, together with other parameter values, used to solve the set of differential equations, are given in Table 1. Source files used in this study can be available at <http://senselab.med.yale.edu/senselab/modeldb>.

### Results

In an initial set of simulations, the value of  $\bar{g}_{TRP}$  was arbitrarily set to be  $0.03 \text{ mS/cm}^2$ . The initial values of the variables,  $V$ ,  $m$ ,  $h$  and  $n$  are  $-71 \text{ mV}$ ,  $0.038$ ,  $0.69$ , and  $0.159$ , respectively. Under these conditions, when amplitude and frequency of the externally-applied voltage (*i.e.*,  $V_{ext}$ ) was set to be  $8 \text{ mV}$  and  $0.3 \text{ Hz}$ , repetitive bursts of action potentials (APs) were readily generated in this model neuron (Fig. 2). The firing of APs in response to sinusoidal change in externally-applied voltage was found to be phase-locked. The appearance of bursting APs in response to sinusoid voltage tends to be entrained by the cycle stimulation with a frequency of  $0.3 \text{ Hz}$ . As the resting potential was sinusoidally changed, such bursting pattern with a 19:1 phase locking was clearly seen in this simulation. That is, nineteen APs with the same waveform can be generated for each cycle stimulation. The firing pattern was also found to vary with changes in the frequency of sinusoid voltage. When the frequency reached to  $10 \text{ Hz}$ , the synchronous firing of APs in a 1:1 fashion was observed. Of note, as the value of  $\bar{g}_{TRP}$  was arbitrarily increased to  $0.06 \text{ mS/cm}^2$  with a fixed frequency of  $0.3 \text{ Hz}$ , the bursting frequency of APs was greatly increased and a 42:1 phase-locking pattern emerged, although the shape for each single AP remains unchanged. The results indicate that as low-frequency sinusoidal voltage (*i.e.*, from  $0.01$  to  $5 \text{ Hz}$ ) is applied,  $\bar{g}_{TRP}$  of varying conductances can reach activation threshold of AP, thereby leading to a significant alteration of the  $p:q$  phase-locking patterns in this model neuron where  $I_{TRP}$  was incorporated. Therefore, the simulation results show that the pattern of entrainment can vary with changes in the activity of TRP-like channels.

Figure 3 showed the evolution of interspike interval (ISI) with change in the number of intervals ( $n$ ), when the different values of  $\bar{g}_{TRP}$  ( $0.03$  and  $0.06 \text{ mS/cm}^2$ ) are applied to the model neuron. The inter-

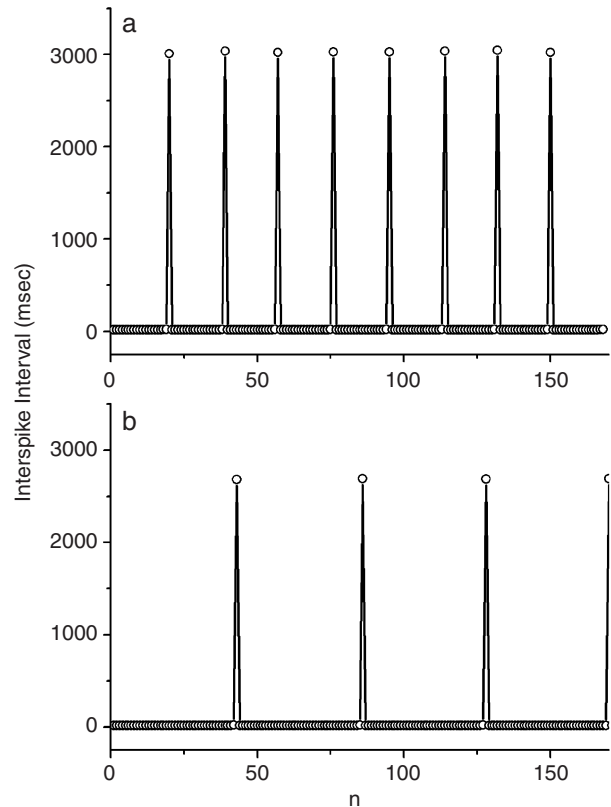


Fig. 3. Interspike interval (ISI) versus interval number. ISI map derived from electrical firing of model neuron in which the different value of  $\bar{g}_{TRP}$  were included. In (a) and (b),  $\bar{g}_{TRP}$  was set to be  $0.03$  and  $0.06 \text{ mS/cm}^2$ , respectively. Notably, the peak value of ISI is greater in (a) than in (b), although the pattern of ISI map between them was found to be similar.

spike intervals are measured when the membrane potential crosses a threshold (at  $-50 \text{ mV}$ ) with a positive derivative. As stimulus frequency of  $0.3 \text{ Hz}$  with a fixed amplitude of  $8 \text{ mV}$  was applied, the ISI pattern, which exhibited to be periodic in the phase-locking pattern, remains similar between these two conditions (Fig. 3). However, the maximal values of ISIs are greater with  $\bar{g}_{TRP} = 0.03 \text{ mS/cm}^2$  than with  $\bar{g}_{TRP} = 0.06 \text{ mS/cm}^2$ . The model neuron thus tends to shorten ISIs as  $\bar{g}_{TRP}$  was increased. The results suggest that activation of TRP-like channel can result in facilitation of bursting activity induced by low-frequency sinusoidal voltage.

In another series of simulations, applying high-frequency voltages (*e.g.*,  $60 \text{ Hz}$ ), we could found a chaotic pattern of AP firing when the amplitude and frequency of external voltage were set to be  $2 \text{ mV}$  and  $60 \text{ Hz}$  (Fig. 4). Interestingly, when the value of  $\bar{g}_{TRP}$  was elevated from  $0.015$  to  $0.03 \text{ mS/cm}^2$ , the increased firing rate was found to be accompanied by the conversion from an irregular to a regular discharge pattern.

Figure 5 illustrates the evolution of ISI as a

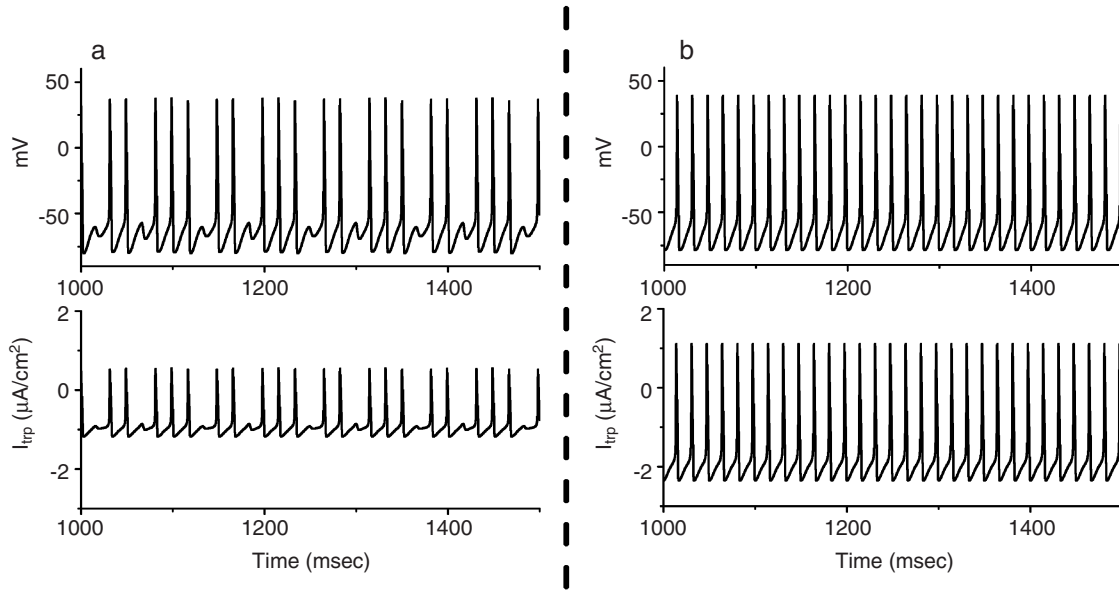


Fig. 4. Effect of  $I_{TRP}$  on modified HH model during exposure to high-frequency sinusoidal voltage. The amplitude and frequency of external voltage were set to be 2 mV and 60 Hz, respectively. In (a) and (b),  $\bar{g}_{TRP}$  is 0.015 and 0.03 mS/cm<sup>2</sup>, respectively. In (a), the entrainment pattern in (a) tends to be chaotic with 3:2/4:3. However, when  $\bar{g}_{TRP}$  was increased to 0.06 mS/cm<sup>2</sup>, the firing of APs becomes regular. Time course of  $I_{TRP}$  is illustrated in the lower part of each panel. Notably, the amplitude of  $I_{TRP}$  in (a) is lower than in (b).

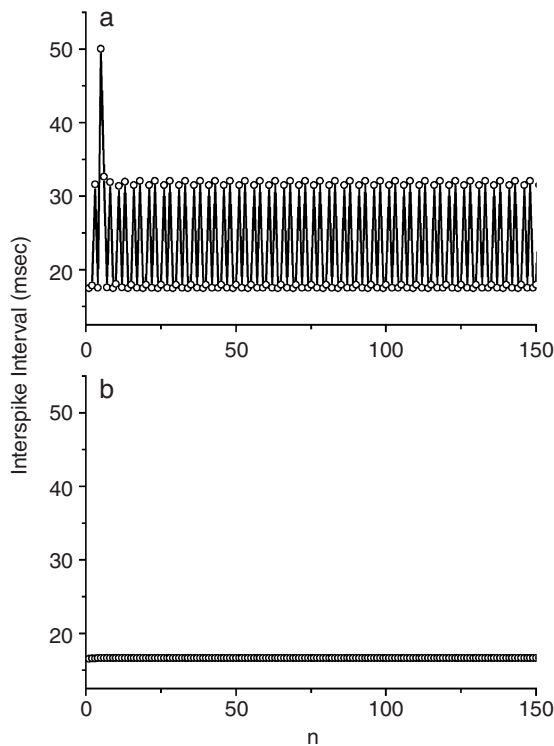


Fig. 5. ISI map obtained when high-frequency electrical potential was applied to model neuron. The amplitude and frequency of external voltage were set to be 2 mV and 60 Hz, respectively. Notably, the duration of ISIs is not constant in (a) where the value of  $\bar{g}_{TRP}$  is 0.015 mS/cm<sup>2</sup>; however the duration of ISIs shown in (b) where  $\bar{g}_{TRP} = 0.03$  mS/cm<sup>2</sup> remains unchanged.

function of changes in  $n$  as  $\bar{g}_{TRP}$  was set to be 0.015 and 0.03 mS/cm<sup>2</sup>. When  $\bar{g}_{TRP}$  was 0.015 mS/cm<sup>2</sup> with a high frequency of sinusoidal voltage (60 Hz), the ISIs became out of order. The maximum values of ISIs turned out to vary irregularly. The entrainment pattern of 3:2 was found to alternate with that of 4:3. However, as  $\bar{g}_{TRP}$  was increased to 0.03 mS/cm<sup>2</sup>, the ISI was converted to be constant as the number of interval was increased. Therefore, it is possible that as the value of  $\bar{g}_{TRP}$  is properly increased, electrical pattern can be converted from irregular to regular pattern during the exposure to high-frequency sinusoidal voltage.

## Discussion

The output of many mammalian neurons is not a single action potential, but a burst of action potentials. Critical to the importance of burst firing is the fidelity of information transfer during a burst of action potentials. Burst firing has been previously shown to increase the probability of long-term potentiation induction in CA1 pyramidal neurons, suggesting that information storage may be enhanced during this mode of action potential firing. In terms of neuropeptide release, burst stimulation was also noted to be more effective than constant-frequency stimulation (6). Thus, it is likely that sinusoidal voltage with varying ranges of low frequency may have a significant impact on neuronal function, as it alters

the pattern of burst firing in model neuron. This simulation also suggest that burst firing in small-diameter peripheral sensory neurons can be facilitated by the activation of TRP-like channel.

Changes in the extracellular (*e.g.*, VR1 receptor activation) or intracellular environment (gene expression), and in externally-applied voltage, in many cases, can be reflected in an alteration of spontaneous firing properties such as the frequency and firing pattern of excitable cells and also in changes in the shape of their action potentials. Electrical stimulation with different frequencies was demonstrated to affect the release of many neuropeptides from neurons or neuroendocrine cells *in vivo* (8, 10). Electrical stimulation of acupuncture needles which activates afferent nerve fibers (*i.e.*, electro-acupuncture) was also recently reported to mimic the application of sinusoidal voltage to the HH model neuron (15). Our simulations extend the results to show that activation of  $I_{TRP}$  may qualitatively alter different firing pattern of APs in model neuron exposed to sinusoidal voltage with varying frequencies.

The mathematical model presented here may provide a general rule in determining the relationship between the property and role of individual ion channel (*e.g.*, TRP channels). This approach will be useful, especially because an extremely large diversity of ion channel properties is expected from the presence of multiple pore forming and accessory subunits and alternative splicing of transcripts in various animal species. Our simulations also led us to propose that either different expression levels of the TRP-like channels or gain-of-function mutations in these channels may affect the firing pattern in capsaicin-sensitive sensory neurons to some extent.

A recent study showed that as activation and inactivation parameters in response to prolonged depolarization were altered, there was an emergence of periodicity in membrane potential from model neuron (13). As the activity of TRP-like channel is properly elevated, membrane would be expected to be depolarized due to influx of a large amount of cations into the cell. It thus remains to be further evaluated whether modification in activation and inactivation kinetics of  $I_{Na}$  can influence electrical behavior of APs in neurons exposed to oscillating external voltage.

An important feature of the simulation is that it can provide insight about the hypothesized mechanisms involved in excitation in a way that is not practical with real experiments. Therefore, we expect that mathematical approach used here may help to select effective paths for experiments that would otherwise require enormous time. The model helps us to make predictions that can be tested experimentally and more importantly, to facilitate the experimental search.

This model may also explore the different levels of TRP gene expression not yet achieved in experiments. Genetic engineering techniques have been recently employed to clone, modify, and characterize the gating mechanisms of many different types of ion channels (9). In this way, it may be possible to score the overall effect of a mutation of TRP channels and to build predictive links between genotype and phenotype.

### Acknowledgments

This work was partly supported by grants from the National Science Council (NSC-94-2320B-006-019), and the Program for Promoting Academic Excellence and Developing World Class Research Centers, Ministry of Education, Taiwan, ROC. The authors would also like to thank the support from Cardiac Electrophysiology and Systems-biology Center, National Cheng Kung University Medical Center, Tainan, Taiwan, ROC.

### References

1. Bölcskei, K., Helyes, Z., Szabó, Á., Sándor, K., Elekes, K., Németh, J., Almási, R., Pintér, E., Pethő, G. and Szolcsányi, J. Investigation of the role of TRPV1 receptors in acute and chronic nociceptive processes using gene-deficient mice. *Pain* 117: 368-376, 2005.
2. Caterina, M.J. Transient receptor potential ion channels as participants in thermosensation and thermoregulation. *Am. J. Physiol. Regul. Integr. Comp. Physiol.* 292: R64-R76, 2007.
3. de Levie, R. Advanced Excel® for scientific data analysis. Oxford University Press, New York, Inc., New York, 2004.
4. Ermentrout, G.B. *Simulating, Analyzing, and Animating Dynamical System: A Guide to XPPAUT for Researchers and Students*. Philadelphia, USA Society for Industrial and Applied Mathematics (SIAM), 2002.
5. Gunthorpe, M.J., Benham, C.D., Randall, A. and Davis, J.B. The diversity in the vanilloid (TRPV) receptor family of ion channels. *Trends. Pharmacol. Sci.* 23: 183-191, 2002.
6. Han, J.S. Acupuncture: neuropeptide release produced by electrical stimulation of different frequencies. *Trends Neurosci.* 26: 17-22, 2003.
7. Hille, B. *Ion Channels of Excitable Membranes*, 3rd Ed., Sunderland, MA: Sinauer Massachusetts, USA 2001.
8. Hodgkin, A.L. and Huxley, A.F. A quantitative description of membrane current and its application to conduction and excitation in nerve. *J. Physiol.* 117: 500-544, 1952.
9. Kanani, S., Pumar, A. and Krinsky, V. Genetically engineered cardiac pacemaker: stem cells transfected with HCN2 gene and myocytes-a model. *Phys. Lett. A* 372: 141-147, 2008.
10. Liu, L., Lo, Y., Chen, I. and Simon, S.A. The responses of rat trigeminal ganglion neurons to capsaicin and two nonpungent vanilloid receptor agonists, olvanil and glyceryl nonamide. *J. Neurosci.* 17: 4101-4111, 1997.
11. Lo, Y.C., Wu, J.R., Wu, S.N. and Chen, I.J. Glyceryl nonivamide: a capsaicin derivative with cardiac calcitonin gene-related peptide releasing,  $K^+$  channel opening and vasorelaxant properties. *J. Pharmacol. Exp. Ther.* 281: 253-260, 1997.
12. Lv, Y.G. Theoretical evaluation on monitoring hypothermic anesthesia by the electrical response of human skin neurons. *Forsch. Ingenieurwes.* 71: 79-88, 2007.
13. Majumdar, S. and Sikdar, S.K. Periodicity in  $Na^+$  channel proper-

- ties alters excitability of a model neuron. *Biochem. Biophys. Res. Commun.* 359: 908-914, 2007.
14. Sándor, K., Helyes, Z., Gyires, K., Szolcsányi, J. and Lászió, J. Static magnetic field-induced anti-nociceptive effect and the involvement of capsaicin-sensitive sensory nerves in this mechanism. *Life Sci.* 81: 97-102, 2007.
  15. Wang, J., Si, W., Chie, Y. and Fei, X. Spike trains in Hodgkin-Huxley model and ISIs of acupuncture manipulations. *Chaos, Solitons & Fractals* 36: 890-900, 2008.
  16. Wang, Y.J., Lin, M.W., Lin, A.A. and Wu, S.N. Riluzole-induced block of voltage-gated Na<sup>+</sup> current and activation of BK<sub>Ca</sub> channels in cultured differentiated human skeletal muscle cells. *Life Sci.* 82: 11-20, 2008.
  17. Wu, S.N. Simulations of the cardiac action potential based on the Hodgkin-Huxley kinetics with the use of Microsoft Excel spreadsheets. *Chinese J. Physiol.* 47: 15-22, 2004.
  18. Wu, S.N. and Chang, H.D. Diethyl pyrocarbonate, a histidine-modifying agent, directly stimulates activity of ATP-sensitive potassium channels in pituitary GH<sub>3</sub> cells. *Biochem. Pharmacol.* 71: 615-623, 2006.
  19. Wu, S.N., Chen, B.S., Lin, M.W. and Liu, Y.C. Contribution of slowly inactivating potassium current to delayed firing of action potentials in NG108-15 neuronal cells: experimental and theoretical studies. *J. Theor. Biol.* 252: 711-721, 2008.
  20. Zhu, W., Xu, P., Cuascat, F.X., Hall, A.K. and Oxford, G.S. Activin acutely sensitizes dorsal root ganglion neurons and induces hyperalgesia via PKC-mediated potentiation of transient receptor potential vanilloid I. *J. Neurosci.* 27: 13770-13780, 2007.